Analysis of Mechanical Properties of Trapezoidal Polypyrrole Actuator

Kai Ma [1], Shuangjie Liu [1], Yongping Hao [1], Yi Cao[1]

[1] *School of Equipment Engineering, Shenyang Ligong University, Shenyang, Liaoning, China*

Abstract

To solve the problem of poor mechanical properties of rectangular polypyrrole actuator, a trapezoidal polypyrrole actuator is designed in this paper. After electrifying the actuator, the force generated by ion transfer is equivalent to the concentrated load F at the free end, The surface stress distribution and end displacement of trapezoidal polypyrrole actuator with different free end widths were analyzed by using the pure bending theory of cantilever beam and finite element simulation method. The results show that the surface stress attenuation of the trapezoidal polypyrrole actuator is obviously reduced and its mechanical properties are improved. Meanwhile, the end displacement of the trapezoidal polypyrrole actuator with α=0.2 is 24.6% higher than that of the rectangular polypyrrole actuator with the same size.

Keywords

Trapezoidal structure; Polypyrrole; Cantilever beam; The finite element

1. Introduction

Polypyrrole actuator is a kind of conductive polymer with excellent performance, due to its advantages of large output displacement, small volume, good reversibility and good biocompatibility, it has been widely concerned by researchers [1]. Polypyrrole actuators are also called "artificial muscles" [2−4],because of their similar motion mode to animal muscles under the action of driving voltage. They have a wide application prospect in bionics, actuators, sensors, biomedicine and other fields[5−7].

Researchers have done a lot of research work on the preparation, driving principle, mathematical modeling, performance testing and application of polypyrrole actuators[8， 9]. Study shows that although polypyrrole actuators under low driving voltage can be output at the end of large displacement, but the poor mechanical properties, in order to improve the mechanical properties of polypyrrole actuator, this paper designs a trapezoidal structure of polypyrrole actuators, and through the theoretical calculation and ANSYS finite element simulation method of combining the analysis of the surface stress distribution.

2. Structure and working principle of polypyrrole actuator

2.1. Structure of polypyrrole actuator

The polypyrrole actuator has a multi-layer structure, and Figure 1 is the schematic diagram of the three-layer polypyrrole actuator. The middle layer is polyvinylidene fluoride (PVDF) film, non-conductive, porosity 0.45μm, thickness is about 110μm. Its function is to store a solution of propylene carbonate doped with a concentration of 0.5mol/L LiTFSI(bis trifluoromethane sulfonimide lithium) to provide sufficient ions for the polypyrrole actuator to work in air and water; The secondary outer layer

ISCIPT2022@7th International Conference on Computer and Information Processing Technology, August 5-7, 2022, Shenyang, China
EMAIL: 982750993@qq.com (Kai Ma.); Corresponding author: shuangjieliu@126.com (Shuangjie Liu); yphsit@126.com (Yongping Hao); 243641220@qq.com (Yi Cao)

is a conductive metal coating, by magnetron sputtering on both sides of PVDF film, the layer of Cu-Sn alloy film with a thickness of about 50nm is sputtered to form a conductive plane as the electrode of polypyrrole electrochemical deposition. Meanwhile, the conductivity between the PPy layer and electrolyte can also be improved; In the outermost layer, a polypyrrole layer with a thickness of about 30μm was deposited on the conductive plane by electrochemical deposition method. Ions can migrate in the polypyrrole layer after electrification.

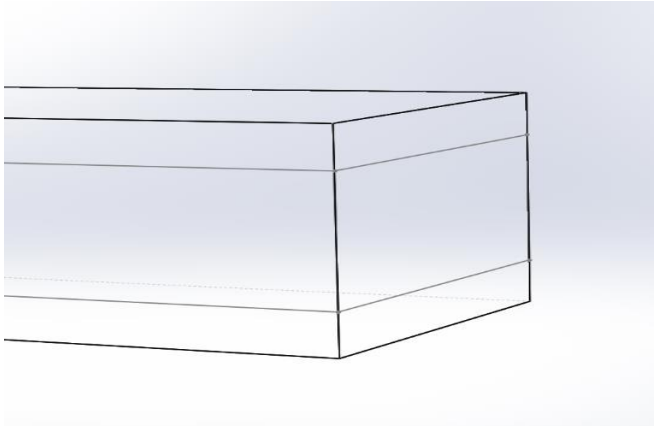

Figure 1: Structure diagram of three layers polypyrrole actuator

2.2. Working principle

The diffusion rate of anion ($TFSI^-$) in the three-layer structure of polypyrrole actuator is much higher than that of cation (Li^+), so the polypyrrole actuator is driven by anion. As shown in Figure 2, when a voltage is applied to the polypyrrole actuator, the polypyrrole layer connected to the positive pole of the power supply reacts with oxidation and loses electrons. In order to maintain electrically neutral anion ($TFSI^-$) stored in the PVDF layer moves to the anode, and the anode expands due to the anionic volume obtained. The polypyrrole layer connected to the negative pole of the power supply is reduced and the $TFSI^-$ anion moves towards the anode. The displacement of anions also carried away solvent molecules and caused volume shrinkage at the cathode. Therefore, the polypyrrole actuator is macroscopically bent towards the cathode after electrification [10].

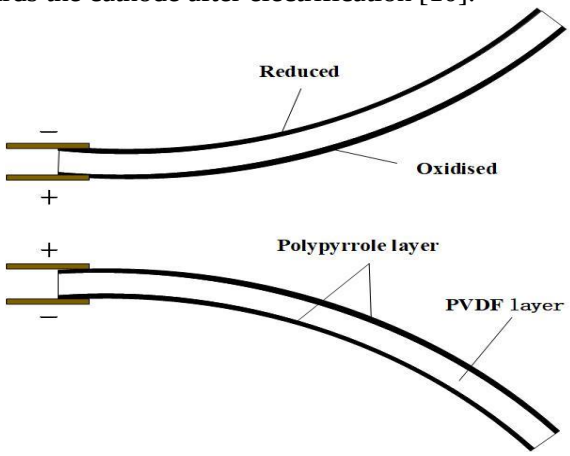

Figure 2: Schematic diagram of bending principle

3. Analysis of mechanical properties of trapezoidal polypyrrole actuator

The actuator is caused by the expansion or contraction of the polypyrrole layer due to ion migration, and the bending stress inside the actuator is related to excitation voltage, charge density, ion concentration and other parameters [11]. In this paper, a mathematical model is established based on the pure bending theory of cantilever beam. The force generated by ion transfer after the actuator is energized is equivalent to the concentrated load F at the free end. In this paper, the structure of the

polypyrrole actuator was optimized to improve the surface stress distribution of the actuator and improve the end output displacement. The schematic diagram of the trapezoidal polypyrrole actuator is shown in Figure 3 below.

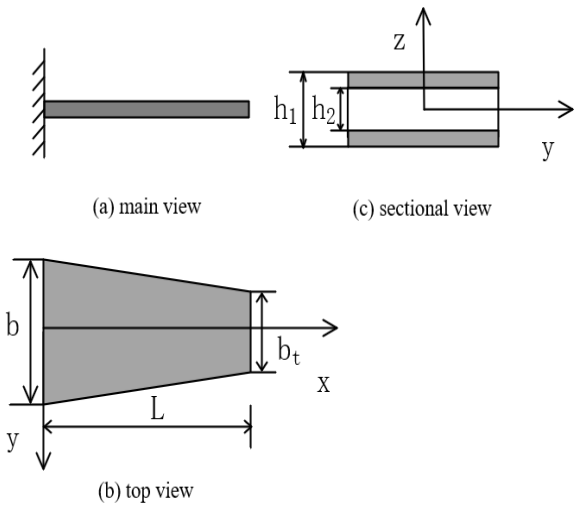

Figure 3: Schematic diagram of trapezoidal polypyrrole actuator

As shown in the Figure 3(c), the trapezoidal polypyrrole actuator is a three-layer composite structure, the middle layer is polyvinylidene fluoride (PVDF), and the outermost layer is polypyrrole (PPy). In mechanical analysis, PVDF and PPy are considered to be isotropic materials, and Young's modulus and Poisson's ratio remain unchanged during bending deformation. Since the thickness of the sputtering metal layer is only 50nm, far less than the thickness of the actuator, the impact of the sputtering layer on the stiffness of the actuator is ignored [8]. In Figure 3, b is the width of the fixed end of the actuator, b_t is the width of the free end of the actuator, L is the length of the actuator, h_1 is the thickness of the actuator, and h_2 is the thickness of PVDF layer.

As shown in Figure 3(c), the y-axis is established along the neutral axis of the section, ρ represents the curvature radius of the neutral layer, and the longitudinal normal strain on the section of the actuator can be expressed as:

$$\varepsilon = \frac{z}{\rho} \tag{1}$$

In the elastic range, the normal bending stress of PPy layer and PVDF layer can be obtained by Hooke's law:

$$\sigma_{PPy} = E_{PPy}\frac{z}{\rho} \tag{2}$$

$$\sigma_{PVDF} = E_{PVDF}\frac{z}{\rho} \tag{3}$$

Only the bending moment exists in the actuator section, which can be obtained according to euler-Bernoulli beam theory:

$$M = EI\frac{1}{\rho} \tag{4}$$

By substituting Equations (2) and (3) into Equation (4), the bending normal stress of PPy layer and PVDF layer can be obtained:

$$\sigma_{PPy} = \frac{ME_{PPy}z}{EI} \tag{5}$$

$$\sigma_{PVDF} = \frac{ME_{PVDF}z}{EI} \tag{6}$$

In order to quantitatively characterize trapezoidal structures with different free-end widths, a coefficient α is introduced:

$$\alpha = \frac{(b - b_t)}{L} \tag{7}$$

Along the positive direction of x-axis, actuator widths at different x points are expressed as:

$$b(x) = b - \alpha x \tag{8}$$

As shown in Figure 3(c), Y-axis is the neutral axis of the actuator section, and the moment of inertia of each layer is:

$$I_{PVDF} = \frac{b(x)h_2^3}{12} \tag{9}$$

$$I_{PPy} = \frac{b(x)(h_1^3 - h_2^3)}{12} \tag{10}$$

When $n = \frac{E_{PPy}}{E_{PVDF}}$, the equivalent moment of inertia of the actuator is expressed as:

$$I_z = I_{PVDF} + \frac{E_{PPy}}{E_{PVDF}} I_{PPy} = \frac{A_1 b(x)}{E_{PVDF}} \tag{11}$$

The bending stiffness of the actuator is:

$$EI = E_{PVDF} I_{PVDF} + E_{PPy} I_{PPy} = A_1 b(x) \tag{12}$$

$$A_1 = \frac{E_{PVDF} h_2^3 + E_{PPy}(h_1^3 - h_2^3)}{12} \tag{13}$$

Assuming that the force generated by the free end of the actuator after electrification is F, substitute Equations (11) and (12) into equations (5) and (6) to obtain:

$$\sigma_{PPy} = \frac{nMz}{I_z} = \frac{E_{PPy} F(L-x)z}{A_1 b(x)} = \frac{E_{PPy} F(L-x)z}{A_1(b - \alpha x)} \tag{14}$$

$$\sigma_{PVDF} = \frac{Mz}{I_z} = \frac{E_{PVDF} F(L-x)z}{A_1 b(x)} = \frac{E_{PVDF} F(L-x)z}{A_1(b - \alpha x)} \tag{15}$$

Where EPPy and EPVDF represent the Young's modulus of polypyrrole layer and PVDF layer respectively, z represents the distance from the neutral axis, L and b represent the length and fixed end width of the actuator respectively.

According to Equations (11) and (12), the equivalent moment of inertia and sectional stiffness of the trapezoidal polypyrrole actuator are no longer constants along the x-axis, but functions of x. For Equation (14), the surface stress of the actuator is no longer linearly attenuated along the x-axis. With the increase of α, the surface stress attenuation of the actuator also slows down. The trapezoidal structure is beneficial to improve the surface stress distribution and load capacity of the actuator.

4. Finite element analysis

The material parameters and structural parameters of the trapezoidal polypyrrole actuator are shown in Table 1 below. A simulation model is established in ANSYS. The fixed end uses fixed constraints, and the z-direction concentrated load is applied on the free end face, F= -2mN. The surface stress distribution and end displacement of trapezoidal polypyrrole actuators with different free end widths were investigated.

Table 1

Trapezoidal polypyrrole execution equipment material parameters and structural parameters

	PPy layers	PVDF layers
Length/mm	20	20

Thickness/mm	0.03	0.11
Fixed end Width/mm	5	5
Young's modulus/MPa	80	440
Density/kg · m-3	1150	1150
Poisson's ratio	0.25	0.25

Under the action of vertically downward concentrated load F= -2mN applied at the free end, the surface stress distribution curve was drawn along the axis of the upper surface of the trapezoidal polypyrrole actuator, as shown in Figure 4. With the increase of α, that is, the width of the free end decreases, the stress attenuation on the upper surface of the actuator gradually slows down. When α=0, that is, the stress value at the central point of the axis on the upper surface of the rectangular polypyrrole actuator is 0.37327MPa, and when α=0.2, the stress value at this point is 0.62785MPa, which is 68.2% higher than that at the point of the rectangular structure. This is consistent with the above theoretical analysis results, which proves that the mechanical properties of polypyrrole actuator with trapezoidal structure are improved.

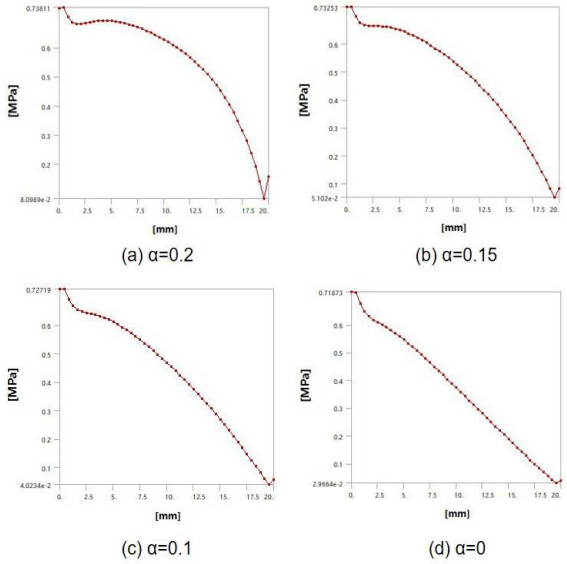

Figure 4: Simulation results of axial stress distribution of trapezoidal polypyrrole actuator with different free-end widths

Figure 5 shows the simulation results of the actuator's end displacement. According to the simulation results, it can be seen that under the same load mentioned above, the actuator's end position also increases with the increase of α. In Figure 5(d), the end displacement of the actuator with α=0 is 14.433mm, and that of the actuator with α=0.2 in Figure 5(a) is 19.145mm, which is 24.6% higher than that of the rectangular polypyrrole actuator.

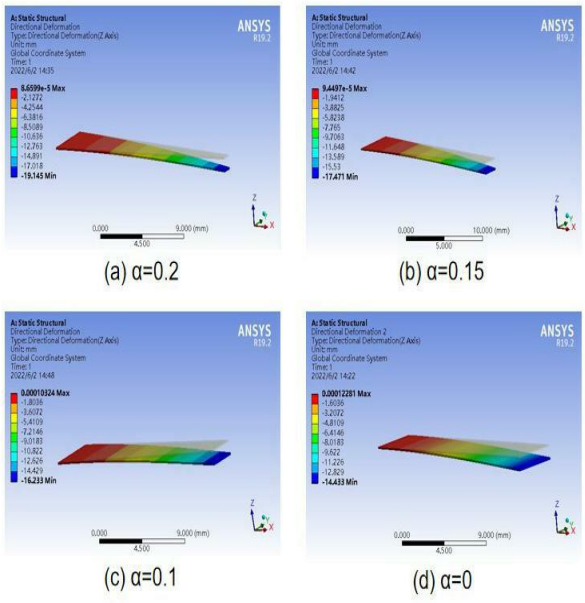

Figure 5: Simulation results of end displacement of trapezoidal polypyrrole actuator with different free end widths

5. Conclusion

In this paper, the polypyrrole actuator with trapezoidal structure is designed by optimizing the structure of the polypyrrole actuator, and the force generated by ion transfer after the actuator is energized is equivalent to the concentrated load F at the free end. Then the surface stress distribution and end displacement of trapezoidal polypyrrole actuator with different free end widths are analyzed by using the mathematical model of pure bending theory of cantilever beam and ANSYS finite element simulation. The theoretical and simulation results show that with the decrease of the width of the free end, that is, with the increase of α, the surface stress of the actuator decreases along the axis. Under the action of concentrated load F= -2mN on the free end of the polypyrrole actuator, the stress value at the central point of the axis on the upper surface of the trapezoidal polypyrrole actuator with α=0.2 increases by 68.2% compared with that of the rectangular polypyrrole actuator with the same size; The end displacement of the trapezoidal polypyrrole actuator with α=0.2 reaches 19.145mm, which is 24.6% higher than that of the rectangular polypyrrole actuator. This shows that the mechanical properties of the polypyrrole actuator with trapezoidal structure are improved and the end displacement is also improved.

The research content of this paper can provide reference for the structural optimization design of polypyrrole actuator, and the correctness of the theory and simulation results can be verified by experiments in the next step.

6. References

[1] Liu S J, Hao Y P. Application of conductive polymer polypyrrole in actuator [J]. Journal of ordnance equipment engineering,2020,41(08):138-141.

[2] Rahim Mutlu,Gursel Alici. Artificial muscles with adjustable stiffness[J]. Smart Materials and Structures,2010,19(4).

[3] Gaoyi Han,Gaoquan Shi. Conducting polymer electrochemical actuator made of high-strength three-layered composite films of polythiophene and polypyrrole[J]. Sensors & Actuators: B. Chemical,2004,99(2).

[4] Li X F, Liang S M, Li Y F, Wang Y X, Xu J. Research progress of Electroactive Polymer "Artificial muscle" biomimetic Material [J]. Polymer Bulletin,2008(08):134-145.

[5] Liu F L, Ye J T, Hao Y P, Liu S J. Application of conductive polypyrrole in miniature flapping wing aircraft [J]. Materials research and application,2020,14(03):253-258.
[6] Shang X L, Wang X J. Research on sensing characteristics of polypyrrole mechanical sensor [J]. Mechanical and electrical engineering,2017,34(05):450-454.
[7] Lan L Z, Zhang Q, Mao J F, Wang L. Conductive polymer artificial muscle building and biomedical applications [J]. Polymer bulletin, 2021 (9) : 31 to 40. The DOI: 10.14028 / j.carol carroll nki. 1003-3726.2021.09.003.
[8] Gursel Alici,Nam N. Huynh. Predicting force output of trilayer polymer actuators[J]. Sensors & Actuators: A. Physical,2006,132(2).
[9] Gursel Alici,Brian Mui,Chris Cook. Bending modeling and its experimental verification for conducting polymer actuators dedicated to manipulation applications[J]. Sensors & Actuators: A. Physical,2005,126(2).
[10] Yang Fang,Xiaobo Tan,Yantao Shen,Ning Xi,Gursel Alici. A scalable model for trilayer conjugated polymer actuators and its experimental validation[J]. Materials Science & Engineering C,2007,28(3).
[11] Gursel Alici. An effective modelling approach to estimate nonlinear bending behaviour of cantilever type conducting polymer actuators[J]. Sensors & Actuators: B. Chemical,2009,141(1).